Monte Carlo Simulation of Boron Neutron Capture Therapy

QIU You-Heng[1;1)] DENG Li[2] YING Yang-Jun[2] XIAO Gang[2]

1 (Graduate School of China Academe of Engineer Physics, Beijing 100088, China)

2 (Lab. Com. Phy., Institute of Applied Physics and Computational Mathematics, Beijing 100088, China)

Abstract This paper introduces the particle transport process in brain, which is simulated by general Monte Carlo code MCNP. The absorbed dose rates from $^{10}B(n,\alpha)^7Li$, $^{14}N(n,p)^{14}C$, $^1H(n,\gamma)^2D$ and fast neutron elastic scattering reaction are considered. The major contribution to the tumor zone is from the neutron capture reaction of boron. The comparison of the absorbed dose rates from thermal and epithermal neutron indicates that the epithermal neutron beam is more effective than thermal neutron beam in destroying deep-seated tumors, on the contrary, the latter is valid for shallow tumor, e.g. skin cancer. In comparison with deterministic method DOSE program, MCNP code is convenient in simulation of Boron Neutron Capture Therapy.

Key words Monte Carlo simulation, tumor, thermal and epithermal neutron, absorbed dose rate, boron neutron capture therapy

1 Introduction

Boron Neutron Capture Therapy (BNCT) is a technique, which is used in treating brain tumors by artificially loading the tumor tissue with isotope B-enriched compound and subsequently irradiation of brain by low energy neutrons. The technique is based on the $^{10}B(n,\alpha)^7Li$ nuclear reaction emitting alpha particle and ^7Li nuclei with total kinetic energy of 2.79 MeV, which is high enough to destroy the tumor cells [1].

The main nuclear reactions which take place in the brain are $^{10}B(n,\alpha)^7Li$, $^{14}N(n,p)^{14}C$, $^1H(n,\gamma)^2D$ and fast neutron elastic scattering reaction. The absorbed dose rate is the summation of all the individual absorbed dose rates resulting from all above-mentioned reactions. The absorbed dose rate strongly depends on the reaction cross-section and the energy released in the reaction[1].

For BNCT, an adequate thermal neutron field has to be created in boron-labeled tumor cells within a prescribed target volume. This means that for target volumes well below the surface, epithermal beams will generally be best, while for target volumes near the surface, thermal beams will suffice. Thermal neutron irradiations have been used for melanoma treatments in the skin, as well as with open craniotomy for glioma treatments. In general, however, the current trend for treatment of patients with brain tumor is to use epithermal neutron beams[2].

In order to study the superiority of epithermal neutron in treating deep-seated tumor, also the importance of boron concentration, the thermal and epithermal neutron transport processes in brain are simulated by the general Monte Carlo program MCNP-4B[3] for different cases of tumor position. The neutron and gamma energy spectra and the absorbed dose rate distribution in a head phantom are calculated. The results show in good accordance in most cases with the results of M. K. Marashi that were simulated by deterministic method[1]. However, MCNP simulation gives higher thermal neutron flux at deep sites, then the absorbed dose rate is higher than that of multi-group deterministic method. We analyzed this reason. In final, the absorbed dose rates comparison of different tumor depths has been shown.

Received 28 January 2003, Revised 15 May 2003

1) E-mail: hyqiu 821 @ sohu.com

2 Method

Monte Carlo method solves particle transport problems by simulating a great number of individual particles and giving their average behavior. Monte Carlo particle transport process essentially involves the continued tracking of particles through series of discrete event until them either to be thermalized, escape, undergoing collision or to reach neutron energy-limit, weight-limit or time-limit. It has been extensively applied to trial nuclear physics, atomic energy, solid physics, sociology and economics, etc.

MCNP is a general purpose Monte Carlo N-Particle code that can be used for neutron, photon, electron, or coupled neutron/photon/electron transport, including the capability to calculate eigenvalues for critical systems. Point-wise cross-section data are used. Important standard features that make MCNP very versatile and easy to use include a powerful general source, criticality source, and surface source, geometry and output tally plotters, a rich collection of variance reduction techniques, a flexible tally structure, and an extensive collection of cross-section data[3].

In calculating the total and individual absorbed dose rates from the four reactions in the head, the head is simulated by a one-dimension slab of 20cm depth, in Fig.1 an l_2 thick tumor is loaded at a depth of l_1. In our calculation, l_1 takes 1.5cm, 3cm and 5cm, and corresponding l_2 takes 3cm, 5cm and 4.5cm, respectively. The corresponding phantoms are called as shallow, medium and deep tumor model.

The natural elements constituting both the normal tissue and the tumor tissue are supposed to be H, O, N, Na and C with concentrations as listed in Table 1[11]. The concentrations of artificially loaded isotope B in the tumor and normal tissue are assumed to be 30 and 10 ppm, respectively.

Table 1. Concentrations of the elements in the head phantom.

Element	Wt(%)	Atomic density × 10^{24}
H	10.7	6.40×10^{-2}
O	71.4	2.69×10^{-2}
C	12.1	6.02×10^{-2}
Na	4.5	1.18×10^{-2}
N	1.3	5.60×10^{-2}
B-10(normal tissue)	10ppm	5.57×10^{-2}
B-10(tumor)	30ppm	1.67×10^{-2}

The energy of incident epithermal neutron beam is in the range of 3.0354 – 15.034 keV[11]. For thermal beam along the incident direction, it is in the range of 0.05 – 0.1eV, with an intensity normalized to 1 $n\cdot cm^{-3}\cdot s^{-1}$.

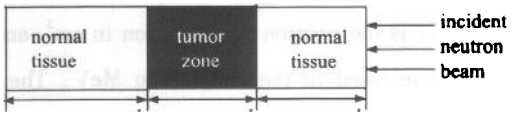

Fig.1. The phantom of BNCT.

3 Calculations of absorbed dose rate

Most of the absorbed dose rates come from the following reactions: $^{10}B(n,\alpha)^7Li$, $^{14}N(n,p)^{14}C$, $^1H(n,\gamma)^2D$, and the elastic scattering reaction. The energy released in each of the reaction other than (n,γ) reaction is deposited locally, whereas the gamma rays from reactions (n,γ) deposit their energy throughout the medium by continuous slowing down of electrons resulting from Compton scattering and photoelectric interaction. A part of the gammas and electrons may escape from the medium, carrying with them the corresponding energy[11]. The absorbed dose rate, due to each nuclear reaction, is considered individually as following:

(a) $^{10}B(n,\alpha)^7Li$ reaction:

^{10}B has a very large thermal neutron capture cross section of 3840 barns. Other than the energy of gamma (0.48MeV), the energy is deposited within 10μm of the reaction site, potentially making the radiation highly cell-selective[4].

$$^{10}B + {}^1n \rightarrow {}^{11}B \begin{cases} \rightarrow {}^4He_2 + {}^7Li_3 + 2.79(MeV)\,(6\%) \\ \rightarrow {}^4He_2 + {}^7Li_3^* + 2.31(MeV)\,(94\%) \\ \qquad\downarrow \\ \qquad {}^7Li_3 + \gamma + 0.48(MeV) \end{cases} \quad (1)$$

(b) $^{14}N(n,p)^{14}C$ reaction:

The total energy about 0.66MeV is released in this reaction, where 0.62MeV is carried by the proton and 0.04 MeV is carried by ^{14}C nuclei. The Kerma rates of the above two reactions in Gy/h are calculated from the following formulation:

$$K(j) = \int_0^{E_{max}} 5.76 \times 10^{-7} \phi(E) \times \sigma(E) \times NT(j) \times E_T dE, \quad (2)$$

where $K(j)$ is the Kerma rate at point j in medium in Gy/h, $\phi(E)$ is the neutron flux at point j in $n \cdot cm^{-2} \cdot s^{-1}$, $NT(j)$ is the number of the specified nuclei/g at point j, $\sigma(E)$ is the neutron cross section in cm^2, and E_T is the energy released in the reaction in MeV. The constant 5.76×10^{-7} is the conversion coefficient, converting MeV/g·s into Gy/h. The energy released in the reaction is deposited locally . Thus with a good approximation it can be equalized to the absorbed dose rate under Charged Particle Equilibrium (CPE) condition, i.e. $D = K$, where D is the absorbed dose rate and K is the Kerma rate[1].

(c) $^1H(n,\gamma)^2D$ reaction:

This reaction is usually called hydrogen capture gamma reaction. The produced gamma takes energy of 2.224 MeV, a fraction of which can escape from the medium. By assuming the CPE condition the absorbed dose rate from the above reaction can be received from the flux-to-dose rate conversion factors. As a matter of fact, the gamma flux multiplied by the flux-to-dose rate conversion factors is the dose rate in rem/h, which is equal to 1000 Gy/h. The conversion factors extracted from ANSI/ANS and ICRP-21 are listed in appendix[3]. The recently published Kerma factor is in ICRU63[5]. In this paper, the absorbed dose rate from all (n,γ) reaction was calculated.

(d) Elastic scattering reaction:

The fast neutron dose is primarily due to elastic neutron collisions with hydrogen, $^1H(n,n')^1H$, and represents 90 % of the adult brain Kerma between energies of ~ 600 eV and ~ 3 MeV. Other neutron reaction, primarily with ^{12}C, ^{16}O, and ^{31}P generally contribute 4 % —8 % to the brain Kerma between ~ 40 eV and ~ 5 MeV, but at certain resonance energies may contribute more[4]. By assuming the CPE condition the absorbed dose rate from fast neutrons is calculated from the following equation:

$$D(j) = 5.76 \times 10^{-7} \times \sum_{i=1}^{N} NT_i(j) \times \iint \phi(E,j) \sigma_{s,i}(E \rightarrow E') \times (E - E') dE dE', \quad (3)$$

where $D(j)$ is the absorbed dose rate at point j in Gy/h, $\phi(E,j)$ is the neutron flux at energy E at point j in $n \cdot cm^{-2} \cdot s^{-1}$, $\sigma_{s,i}(E \rightarrow E')$ is the neutron elastic scattering cross section from energy E to E' MeV in cm^2 for nuclei i, NT_i is the number of nuclei i, and $\Delta E = E - E'$ is the energy lost in one scattering reaction.

Due to the continuous point-wise cross-section was adopted in MCNP code, how to obtain $\sigma_{s,i}(E \rightarrow E')$ is a key. As it is well known, the energy of the recoil neutron approximately obeys the following distribution:

$$f(E \rightarrow E') dE' = \frac{dE'}{(1-\alpha)E}, \alpha E \leqslant E' \leqslant E, \quad (4)$$

$$\sigma_s(E \rightarrow E') = \sigma_s(E) f(E \rightarrow E'), \quad (5)$$

where $\alpha = \left(\frac{A-1}{A+1}\right)^2$, A is the mass of target nucleus, $\sigma_s(E)$ is the neutron total microscopic elastic scattering cross section, and $f(E \rightarrow E')$ is scattering energy transfer function. The energy spectrum of the recoil neutron is uniform for specified target nucleus and incident neutron energy E. So we have

$$\int_{\alpha E}^{E} f(E \rightarrow E')(E - E') dE' = 0.5(1+\alpha)E. \quad (6)$$

And then

$$D(j) = 2.88 \times 10^{-7} \times \sum_{i=1}^{N} NT_i(j) \times \int_0^{E_{max}} \sigma_s(E) \phi(E,j) E(1+\alpha) dE. \quad (7)$$

4 Result and discussion

After an incident epithermal neutron beam radiated the medium tumor model, an energy spectrum of neutrons in the head phantom is produced. The neutron spectrum at three different points in the head phantom is shown in Table.2. It can be seen from the table that, at a distance of 1cm from the scalp surface the epithermal neutron flux is higher than the thermal flux, whereas, at distance 4cm and 15cm it is lower.

Table 2. The flux of thermal and epi-thermal neutron at three different depths.

Depth/cm	Φ_{th}/n·cm^{-2}·s^{-1}	Φ_{epi}/n·cm^{-2}·s^{-1}
1	1.192688	2.37240
4	1.748584	0.86915
15	0.136651	0.01509

As soon as the epithermal neutrons enter into the

head phantom, they are scattered into low energy neutron. As it is expected in Fig.2, the thermal group neutrons enrich in tumor zone.

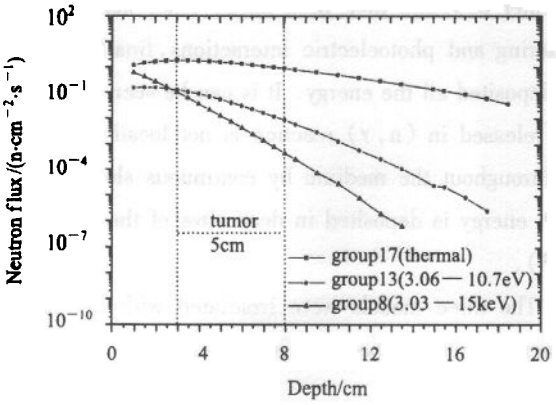

Fig.2. Distribution of neutron flux with energies of groups 8, 13 and 17 along the head phantom horizontal axis.

In Fig.3, it can be seen that the absorbed dose rate from $^{10}B(n,\alpha)^{7}Li$ reaction due to non-thermal neutrons is

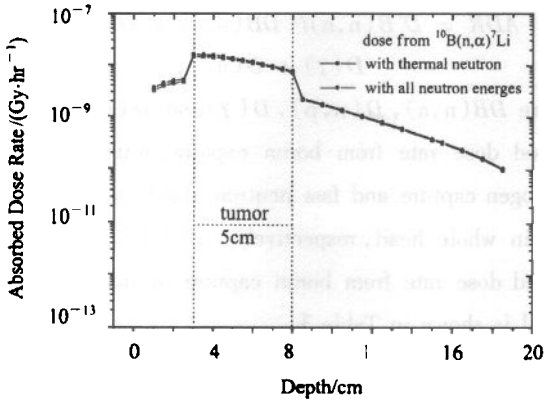

Fig.3. The comparison of Absorbed dose rate along the head phantom due to $^{10}B(n,\alpha)^{7}Li$ reaction with thermal neutron and all neutron energy groups.

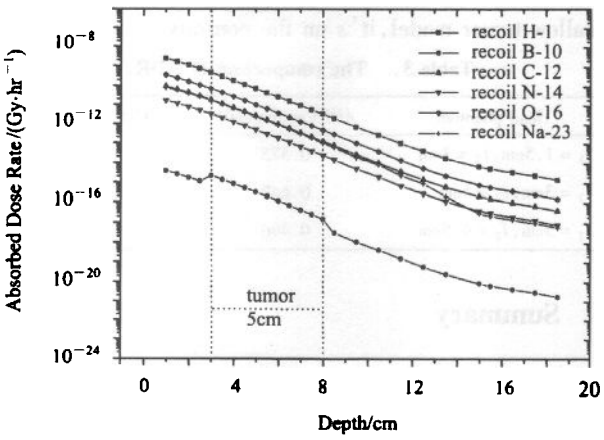

Fig.4. Distribution of absorbed dose rate along the head phantom due to all the neutron elastic scattering reaction.

negligible in comparison with that of thermal neutrons. The same phenomenon appears in nitrogen capture reaction. From the following result, it is seen that the absorbed dose rate in tumor mostly comes from $^{10}B(n,\alpha)^{7}Li$ reaction. That is why the thermal neutron should be enriched in tumor zone; also the concentration of boron in tumor should be higher than that in normal tissue.

In Fig.4 the individual absorbed dose rate from the recoil nuclei (constituting the head phantom) in neutron scattering process is shown. In Fig.5 the absorbed dose

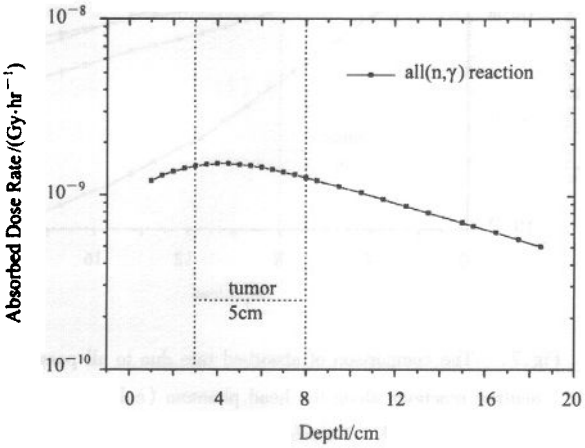

Fig.5. The absorbed dose rate from all the (n,γ) reaction along the head phantom.

rate from (n,γ) is shown. Compared with the result of M. K. Marashi, the curve appears relatively flat. The peak of curve is no more than 4 times of the valley, whereas the peak of curve is 10 times more than the valley in the result of M. K. Marashi.

The comparison of the major absorbed dose rates

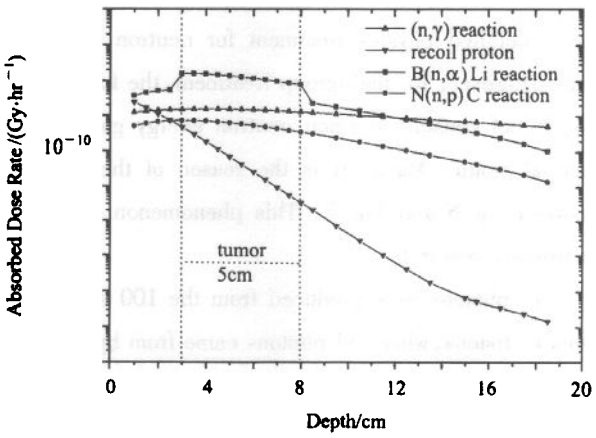

Fig.6. The comparison of absorbed dose rate due to all possible neutron reaction along the depth of medium model with epithermal incident neutron.

from all the nuclear reactions is shown in Fig.6. M. K. Marashi calculated the corresponding absorbed dose rate Fig.7 with the deterministic method code DOSE. The curves in the two figures look almost the same as each other. Some differences appear at near of the deep sites. In comparison with Fig.7, the curves in Fig.6 descend slowly along the depth.

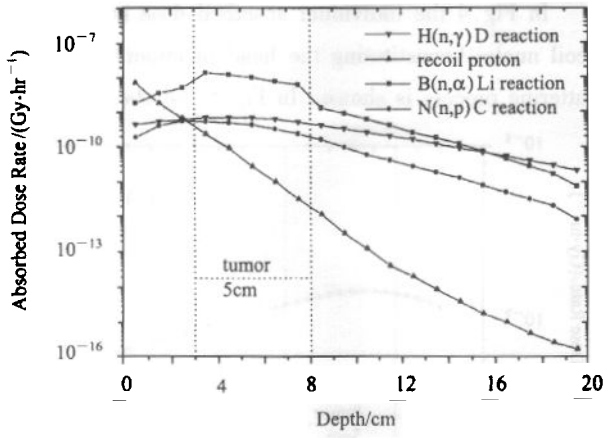

Fig.7. The comparison of absorbed rate due to all possible neutron reactions along the head phantom (calculated by M. K. Marashi. with DOSE).

In order to find the real reason, we tallied 100 source neutrons specially. We found that when the neutron was slowed down into thermal energy range, many up-scattering reactions appeared. A source neutron usually undergoes 200 to 300 collisions before it dies out, and most collisions come from thermal ones. So the thermal neutron flux at deep sites is still relatively high (see Fig.2). Furthermore, boron and nitrogen dose rates mostly come from the reactions with thermal neutron. It can be seen that MCNP has a detailed physics treatment for neutron thermalization. However, for multigroup treatment, the further collision is not considered when neutron energy goes down to thermal group. Maybe it is the reason of the difference between Fig.6 and Fig.7. This phenomenon has existed in primary research.

42 photons were produced from the 100 source neutrons collisions, where 34 photons came from hydrogen capture gamma reaction (with mean free length 21.6cm), 6 photons came from boron capture reaction (with mean free length 10.19cm). 10 photons escaped from medium without any energy lost. After several collisions (less than 8), 20 photons escaped from medium with relatively high energy. The remained 12 photons, after repeating collisions, nearly deposited all their own energy in the medium. Usually the photon flied from one end of the model to the other end, and then flied back. After many Compton scattering and photoelectric interactions, finally, the photon deposited all the energy. It is can be seen that the energy released in (n,γ) reaction is not locally deposited, but throughout the medium by continuous slowing down. Much energy is deposited in deep sites of the model (see Fig 5).

The three models were irradiated with thermal and epithermal neutron beams, respectively. The results were similar to Fig.6.

In order to show the significance and contribution of the boron compound absorbed dose in the tumor with respect to that of the total absorbed dose in the head, a parameter called "Absorbed Dose Ratio" (ADR) is defined as follows:

$$ADR = D'B(n,\alpha)/(DB(n,\alpha) + D(n,p) + D(\gamma) + D(n)), \quad (8)$$

where $DB(n,\alpha)$, $D(n,p)$, $D(\gamma)$ and $D(n)$ are the absorbed dose rate from boron capture, nitrogen capture, hydrogen capture and fast neutron elastic scattering reaction in whole head, respectively. $D'B(n,\alpha)$ is the absorbed dose rate from boron capture in tumor zone, the detail is shown in Table 3

In order to furthest avoid damaging the normal tissue while destroying the tumor; ADR would be better as high as possible. From Table3, it can be seen, for deep and medium model, the ADR of epithermal neutron source is greater than that of thermal neutron source, whereas, for shallow tumor model, it's on the contrary.

Table 3. The comparison of ADR.

Head phantom	*ADR*(epithermal)	*ADR*(thermal)
$l_1 = 1.5$cm, $l_2 = 3$cm	0.575	0.640
$l_1 = 3$cm, $l_2 = 5$cm	0.647	0.569
$l_1 = 5$cm, $l_2 = 4.5$cm	0.496	0.366

5 Summary

As shown in Fig. 4, boron capture reaction mostly comes from thermal neutrons, so ADR is strongly related with the thermal meutron flux in tumor. The incident epithermal neutron has a slowing down process, so the peak

of thermal neutron flux is not at the zone near scalp but tumor zone. If its peak appears in tumor zone, most dose being deposited in the tumor, the scalp tissue is furthest protected while destroying the tumor. So the energy of incident epi-thermal neutron should be changed with the depth of tumor to enrich thermal neutron in the tumor zone.

Also, although the concentration of boron in tumor is far lower than any other elements constituting tumor, the absorbed dose rate from boron capture reaction is much more than other elements. Seeking for right boron compound ensuring the concentration in tumor to be remarkably higher than that in normal tissue is a key to the success of BNCT.

It can be concluded that epithermal neutrons have a greater depth of penetration in tissue and therefore are more effective than thermal neutrons in destroying of the deep seated tumors; thermal neutrons are more effective for the shallow tumor. MCNP can be a very useful tool of simulation of BNCT.

References

1 Marashi M K. Nuclear instrument and Methods in Physics Research, 2000, A **440**:446—452

2 Rorer D, Wambersie A, Whitmore G. et al. edited, Current Status of neutron capture therapy, IAEA, 2001

3 Briesmeister J F. MCNP-A General Monte Carlo Code for N-Particle Transport Code, LA-12625-M (March, 1997)

4 Goorley J T, Kiger W S, Ⅲ, Zamenhof R G. Medical Physics, 2002, **29**:145—156

5 ICRU63, International Commission on Radiation Units and Measurements, 2000, Bethesda, MD

Appendix

Table A1. Photon Flux-to-Dose Rate Conversion Factors.

ANSI/ANS-6.1.1-1977		ICRP-2		ANSI/ANS-6.1.1-1977		ICRP-2	
E /MeV	$DF(E)$ /(rem/h)/(photons/cm^2·s)	E /MeV	$DF(E)$ /(rem/h)/(photons/cm^2·s)	E /MeV	$DF(E)$ /(rem/h)/(photons/cm^2·s)	E /MeV	$DF(E)$ /(rem/h)/(photons/cm^2·s)
0.01	3.96×10^{-6}	0.01	2.78×10^{-6}	1.4	2.51×10^{-6}	3.0	4.00×10^{-6}
0.03	5.82×10^{-7}	0.015	1.11×10^{-6}	1.8	2.99×10^{-6}	4.0	4.76×10^{-6}
0.05	2.90×10^{-7}	0.02	5.88×10^{-7}	2.2	3.42×10^{-6}	5.0	5.56×10^{-6}
0.07	2.58×10^{-7}	0.03	2.56×10^{-7}	2.6	3.82×10^{-6}	6.0	6.25×10^{-6}
0.1	2.83×10^{-7}	0.04	1.56×10^{-7}	2.8	4.01×10^{-6}	8.0	7.69×10^{-6}
0.15	3.79×10^{-7}	0.05	1.20×10^{-7}	3.25	4.41×10^{-6}	10.0	9.09×10^{-6}
0.2	5.01×10^{-7}	0.06	1.11×10^{-7}	3.75	4.83×10^{-6}		
0.25	6.31×10^{-7}	0.08	1.20×10^{-7}	4.25	5.23×10^{-6}		
0.3	7.59×10^{-7}	0.1	1.47×10^{-7}	4.75	5.60×10^{-6}		
0.35	8.78×10^{-7}	0.15	2.38×10^{-7}	5.0	5.80×10^{-6}		
0.4	9.85×10^{-7}	0.2	3.45×10^{-7}	5.25	6.01×10^{-6}		
0.45	1.08×10^{-6}	0.3	5.56×10^{-7}	5.75	6.37×10^{-6}		
0.5	1.17×10^{-6}	0.4	7.69×10^{-7}	6.25	6.74×10^{-6}		
0.55	1.27×10^{-6}	0.5	9.09×10^{-7}	6.75	7.11×10^{-6}		
0.6	1.36×10^{-6}	0.6	1.14×10^{-6}	7.5	7.66×10^{-6}		
0.65	1.44×10^{-6}	0.8	1.47×10^{-6}	9.0	8.77×10^{-6}		
0.7	1.52×10^{-6}	1.0	1.79×10^{-6}	10.0	1.03×10^{-5}		
0.8	1.68×10^{-6}	1.5	2.44×10^{-6}	13.0	1.18×10^{-5}		
1.0	1.98×10^{-6}	2.0	3.03×10^{-6}	15.0	1.33×10^{-5}		

硼中子俘获治疗的蒙特卡罗方法模拟

邱有恒[1;1)] 邓力[2] 应阳君[2] 肖刚[2]

1(中国工程物理研究院北京研究生部 北京 100088)

2(北京应用物理与计算数学研究所计算物理实验室 北京 100088)

摘要 用通用蒙特卡罗程序MCNP模拟了粒子在人脑中的输运过程.吸收剂量率主要来自以下四个反应:$^{10}B(n,\alpha)^{7}Li$,$^{14}N(n,p)^{14}C$,$^{1}H(n,\gamma)^{2}D$,快中子弹性散射反应.对肿瘤区的贡献主要来自硼中子吸收反应.结果表明,超热中子比热中子适合于深肿瘤的治疗,而热中子对浅肿瘤的治疗有优越性,比如皮肤癌.同确定论方法的结果相比,蒙特卡罗方法不失为一种模拟中子俘获治疗的好工具.

关键词 蒙特卡罗模拟 肿瘤 热中子与超热中子 吸收剂量率 硼中子俘获治疗

2003-01-28收稿,2003-05-15收修改稿

1) E-mail:hyqiu821@sohu.com